Conference Proceedings of the Society for Experimental Mechanics Series

Gyaneshwar Tandon *Editor*

Composite, Hybrid, and Multifunctional Materials, Volume 4

Proceedings of the 2014 Annual Conference on Experimental and Applied Mechanics

SEM

Springer

Gyaneshwar Tandon
Editor

Composite, Hybrid, and Multifunctional Materials, Volume 4

Proceedings of the 2014 Annual Conference on Experimental and Applied Mechanics

Springer

Editor
Gyaneshwar Tandon
University of Dayton
Dayton, OH, USA

ISSN 2191-5644 ISSN 2191-5652 (electronic)
ISBN 978-3-319-06991-3 ISBN 978-3-319-06992-0 (eBook)
DOI 10.1007/978-3-319-06992-0
Springer Cham Heidelberg New York Dordrecht London

Library of Congress Control Number: 2014942919

Printed on acid-free paper

Springer is part of Springer Science+Business Media (www.springer.com)

Preface

Experimental Mechanics of Composite, Hybrid, and Multifunctional Materials, Volume 4: Proceedings of the 2014 Annual Conference on Experimental and Applied Mechanics represents one of the eight volumes of technical papers presented at the 2014 SEM Annual Conference & Exposition on Experimental and Applied Mechanics organized by the Society for Experimental Mechanics held in Greenville, SC, June 2–5, 2014. The complete proceedings also includes volumes on: *Dynamic Behavior of Materials*; *Challenges in Mechanics of Time-Dependent Materials*; *Advancement of Optical Methods in Experimental Mechanics*; *Mechanics of Biological Systems and Materials*; *MEMS and Nanotechnology*; *Fracture, Fatigue, Failure and Damage Evolution*; *Experimental and Applied Mechanics*.

Each collection presents early findings from experimental and computational investigations on an important area within Experimental Mechanics, Composite, Hybrid, and Multifunctional Materials being one of these areas.

Composites are increasingly the material of choice for a wide range of applications from sporting equipment to aerospace vehicles. This increase has been fueled by increases in material options, greater understanding of material behaviors, novel design solutions, and improved manufacturing techniques. The broad range of uses and challenges requires a multidisciplinary approach between mechanical, chemical, and physical researchers to continue the rapid rate of advancement.

New materials are being developed from natural sources or from biological inspiration leading to composites with unique properties and more sustainable sources, and testing needs to be performed to characterize their properties. Existing materials used in critical applications and on nanometer scales require deeper understanding of their behaviors and failure mechanisms. New test methods and technologies must be developed in order to perform these studies and to evaluate parts during manufacture and use. In addition, the unique properties of composites present many challenges in joining them with other materials while performing multiple functions.

Dayton, OH, USA

Gyaneshwar Tandon

Contents

Chapter 1
Characterizing the Mechanical Response of a Biocomposite Using the Grid Method

S. Sun, M. Grédiac, E. Toussaint, and J.-D. Mathias

Abstract This work is aimed at determining the mechanical behavior of a biocomposite made of sunflower stem chips and chitosan-based matrix which serves as a binder. The link between global response and local phenomena that occur at the scale of the chips is investigated with a full-field measurement technique, namely the grid method. Regular surface marking with a grid is an issue here because of the very heterogeneous nature of the material. This heterogeneity is due to the presence of voids and the fact that bark and pith chips exhibit a very different stiffness. Surface preparation thus consists first in filling the voids with soft sealant and then painting a grid with a stencil. The grid images grabbed during the test with a CCD camera are then processed using a windowed Fourier transform and both the displacement and strain maps are obtained. Results obtained show that the actual strain fields measured during compression tests are actually heterogeneous, with a distribution which is closely related to the heterogeneities of the material itself.

Keywords Biocomposite • Chitosan • Displacement • Full-field measurement • Grid method • Strain • Sunflower

1.1 Introduction

This work deals with the mechanical characterization of biocomposites made of chips of sunflower stems and a biomatrix derived from chitosan. This biocomposite is developed for building thermal insulation purposes. However, panels made of this material must exhibit minimum mechanical properties to be able to sustain various mechanical loads such as local stress peaks when mounting the panels on walls. This material also features a very low density (nearly 0.17), so it is necessary to study its specific mechanical properties for other applications than thermal insulation only. Such biocomposites are very heterogeneous because stems are made of stiff bark and soft pith.

The stems are generally ground during sunflower harvest and resulting chips are some millimeters in size. A full-field measurement system was therefore applied during compression tests performed on small briquettes made of this material to collect relevant information on the local response of the bark and pith chips. This can help understand local phenomena that occur while testing the specimens, and establish a link with the global response of the tested specimens. The size of the sunflower chips (some millimeters), the amplitude of the local displacement and strain throughout the specimens reached during the tests and the spatial resolution of full-field measurement systems which are nowadays easily available in the experimental mechanics community make it difficult to obtain reliable information on the sought displacement/strain fields. It was therefore decided to employ the grid method to perform these measurements. This technique consists in retrieving the displacement and strain maps assuming that the external surface of the tested specimen is marked with a regular grid. The grids usually employed for this technique are generally transferred using a layer of adhesive [1]. This marking technique could not be used here because of the very low stiffness of the biocomposite. Grids were therefore painted directly on the surface.

S. Sun • M. Grédiac (✉) • E. Toussaint
Clermont Université, Université Blaise Pascal, Institut Pascal, UMR CNRS 6602, BP 10448,
63000 Clermont-Ferrand, France
e-mail: michel.grediac@univ-bpclermont.fr

J.-D. Mathias
IRSTEA, Laboratoire d'Ingénierie pour les Systèmes Complexes, 9 Avenue Blaise Pascal, CS 20085,
63178 Aubière Cedex, France

G. Tandon (ed.), *Composite, Hybrid, and Multifunctional Materials, Volume 4: Proceedings of the 2014 Annual Conference on Experimental and Applied Mechanics*, Conference Proceedings of the Society for Experimental Mechanics Series,
DOI 10.1007/978-3-319-06992-0_1,

The basics of the grid method employed here to measure displacement and strain maps are first briefly given. The marking procedure is then described. Typical results obtained on specimens subjected to compression tests are then presented and discussed.

1.2 Applying the Grid Method to Measure Displacement and Strain Maps

The grid method consists first in marking the surface under investigation in order to track the change in the geometry of the grid while loading increases, and to deduce the 2D displacement and strain fields from these images. Processing grid images consists first in extracting the phases along directions x and y both in the reference and in the current images. Phase extraction is carried out with the windowed Fourier transform (WFT) [2]. The envelope considered in the present study is Gaussian, as in [3]. The displacements u_i i = x, y are obtained from the phase changes $\Delta\Phi_i$, i = x, y between current and reference grid images using the following equation where p is the pitch of the grid:

$$u_i = -\frac{p}{2\pi}\Delta\Phi_i, \quad i = x, y \tag{1.1}$$

The strain components ε_{ij} i = x, y are deduced using the following equation:

$$\varepsilon_{ij} = -\frac{p}{4\pi}\Delta\left(\frac{\partial\Phi_i}{\partial x_j} + \frac{\partial\Phi_j}{\partial x_i}\right), \quad i, j = x, y \tag{1.2}$$

1.3 Description of the Tested Material

Biocomposites studied here are obtained by mixing bark and pith chips, with a biomatrix. Bark provides the main contribution to the mechanical properties of the biocomposite, pith the main thermal insulation properties. A biopolymer based on chitosan is used as a binder [4]. The solvent is merely water containing a low percentage of acetic acid (1 %). In conclusion, it is worth mentioning that this composite material is mainly composed of renewable resources.

1.4 Surface Preparation

There are voids in the biocomposite and some of them are clearly visible to the naked eye on the surface of the specimen, as illustrated in Fig. 1.1.

To avoid any disturbance of the displacement and strain fields measured on the front face of the tested specimen, these voids were filled with a very soft Sikaflex-11FC+ sealant. The impact of this filling material on the response of the specimen is therefore negligible. The surface was then carefully sanded and cleaned. In recent examples of displacement and strain measurements where the grid method was employed, surface marking was generally obtained by transferring a grid, using for instance the technique described in [1]. The problem here is that a layer of adhesive is necessary and this would certainly influence the measured quantity, the stiffness on the substrate being lower than that of the adhesive at some places (pith, voids filled with sealant). This marking technique is therefore not directly applicable here. The grid was painted directly on the surface using a stencil. White paint was first sprayed on the surface of the specimen. The stencil was then placed on this surface and black acrylic ink was sprayed though the stencil with an airbrusher. The lowest size of the square wholes that can be cut in the stencil is the limitation of the technique here. It is equal to 0.4 mm. This finally leads to a grid featuring a frequency of 1.25 lines/mm [5] instead of up to about 10 lines/mm by using the technique described in [1].

Note that the pitch of the grid is not perfectly equal 0.8 mm: it exhibits slight spatial changes which are detected by the WFT (within certain limits). These changes might be considered as caused by a fictitious straining of the tested material beneath the grid. This artifact has been eliminated here by using the procedure described in [3] when processing the grid images.

Fig. 1.1 Front face view of a specimen

1.5 Specimens, Testing Conditions

The specimens were prepared first by moulding small briquettes in which specimens were cut using a saw. The mass percent fraction of chitosan in the biomatrix was equal to 6.25 %. This parameter has an influence on the mechanical response of the specimen [5]. The dimensions of the tested specimens were about $50 \times 80 \times 122$ mm^3. The specimens were subjected to compression tests performed with a 20 kN Zwick-Roell testing machine. The cross-head speed was equal to ~0.02 mm/s. The tested specimens rested on a small plate and the load was applied by imposing a displacement on the upper side. A stiff steel plate was placed on the upper side of the specimen to help obtaining homogeneous imposed displacement and pressure on this side. The lower and upper sides were however not parallel. A 2 mm thin elastomeric sheet was therefore placed between the upper side of the specimen and the moving plate to accommodate displacements imposed on the upper side. The procedure described above was employed to mark the surface with a regular grid after filling the voids with sealant. A Sensicam QE camera was used to grab images of the grid paint on the front face of the specimen during the tests. Nine pixels per period were used to encode one grid pitch.

1.6 Results

A typical mean stress–mean strain curve is shown in Fig. 1.2. A small displacement of the lower support of the specimen being observed, the mean strain is obtained by measuring the average displacement along a line of pixels located 30 pixels under the top face of the specimen to avoid possible edge effects, subtracting it with the average displacement along a line of pixels located 30 pixels above the bottom face of the specimen, and dividing the obtained result by the distance between these two lines. The mean stress is merely the ratio between the applied force and the section of the specimen. In Fig. 1.2, it can be observed that the response is first linear and then non-linear. It is interesting to observe what happens within the material by investigating full-field displacement and strain fields measured on the front face of the specimen.

Figure 1.3 shows a typical vertical displacement field. This displacement is calculated by subtracting the actual displacement and the mean one. It is obtained at the end of the loading phase of the test. As may be seen, the displacement field is irregular. This is due to very local displacement increases due to material heterogeneities. Local strain concentrations can be observed in the vertical strain field shown in Fig. 1.4. On close inspection, they correspond to some zones where the amount of voids is greater than in other zones of the specimen. A more detailed study also shows that the strain level in pith chips is greater than that reached in bark chips, which is certainly due to the difference in stiffness between both constituents [5].

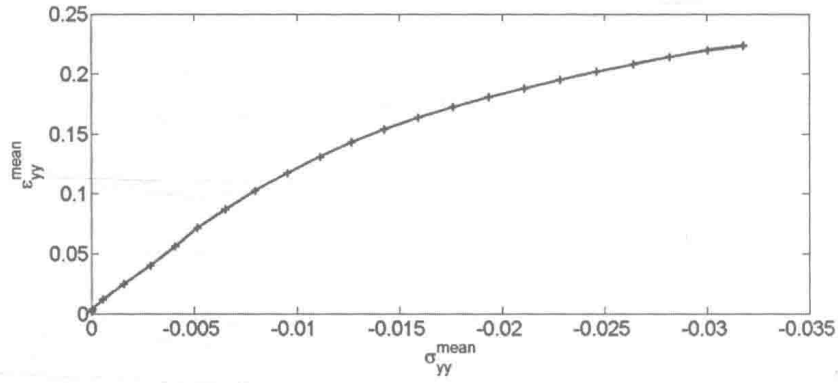

Fig. 1.2 Mean stress–mean strain curve

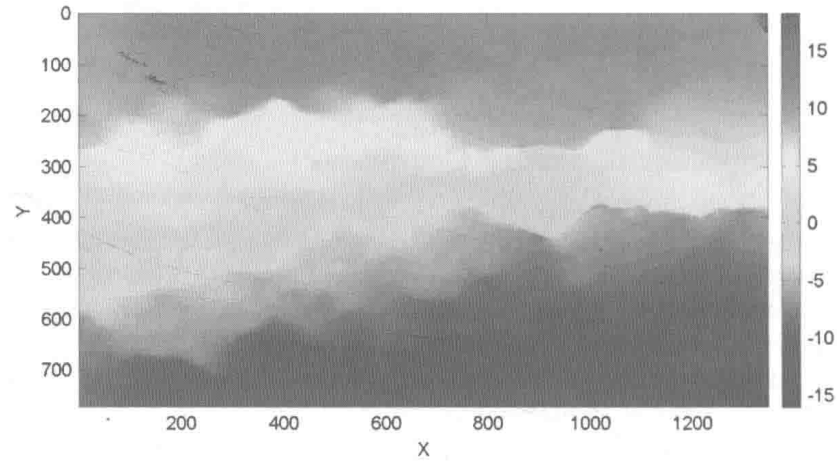

Fig. 1.3 Typical vertical displacement field, in pixels (1 pixel = 40 μm)

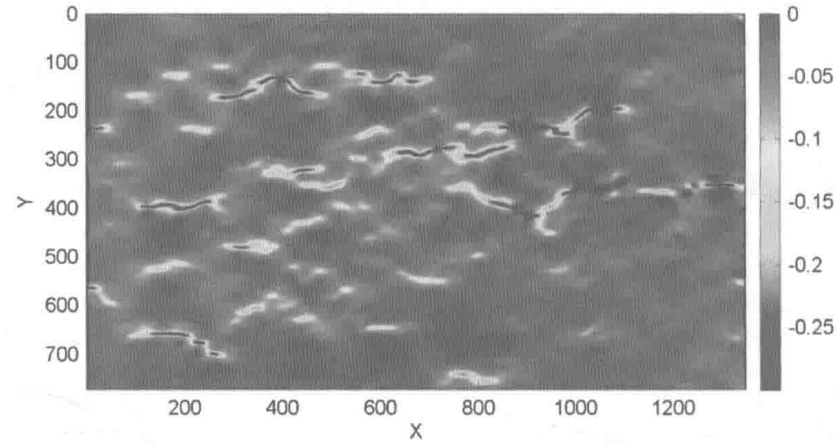

Fig. 1.4 Typical vertical strain field

1.7 Conclusion

The grid method was employed here to characterize the strain field that occurs on the surface of biocomposite specimens. Some very strong heterogeneities are clearly visible. They are closely related to the heterogeneous nature of the material. In particular, the strain level is the highest in zones where voids are present in the material. Even though the measured mechanical characteristics are much greater than the minimum values required for such insulating materials [5], more tests are still necessary to clarify the link between the chitosan volume fraction in the biomatrix, the degree of heterogeneity in the strain field and the strength of the biocomposite. The objective is indeed now to reduce as far as possible the amount of biomatrix in the biocomposite. The reason is that it is the most expensive of all the constituents employed in this material.

References

1. Piro JL, Grédiac M (2004) Producing and transferring low-spatial-frequency grids for measuring displacement fields with moiré and grid methods. Exp Tech 28(4):23–26
2. Surrel Y (2000) Photomechanics, topics in applied physics, vol 77. Springer, Berlin, pp 55–102 (chapter on fringe analysis)
3. Badulescu C, Grédiac M, Mathias J-D (2009) Investigation of the grid method for accurate in-plane strain measurement. Meas Sci Technol 20 (9):095102
4. Patel AK, Michaud P, de Baynast H, Grédiac M, Mathias J-D (2013) Preparation of chitosan-based adhesives and assessment of their mechanical properties. J Appl Polym Sci 127(5):3869–3876. doi:10.1002/app.37685
5. Sun S, Grédiac M, Toussaint E, Mathias J-D, Mati-Baouches N (submitted for publication) Applying a full-field measurement technique to characterize the mechanical response of a sunflower-based biocomposite

Chapter 2
Preliminary Study on the Production of Open Cells Aluminum Foam by Using Organic Sugar as Space Holders

F. Gatamorta, E. Bayraktar, and M.H. Robert

Abstract This work investigates the production of Al foams using organic sugar granulates as space holders. To the Al matrix hollow glass micro spheres were added to constitute a light weight composite material. The process comprises the following steps: mixing of Al powders and organic sugar granulates, compacting of the mixture, heating the green compact to eliminate the sugar and final sintering of the metallic powder. Open spaces left by the volatilization of the sugar granulates constitute a net of interconnect porosity in the final product, which is, therefore, a metallic sponge. It was analyzed the influence of processing parameters in the different steps of production, in the final quality of products. Products were characterized concerning cells distribution and sintering interfaces. Results showed the general viability of producing composites by the proposed technique, based on a simple and low cost procedure.

Keywords Sponge structure • Low cost composites • Organic sugar • Aluminum foam • Sintering

2.1 Introduction

Metal matrix composites (MMCs) are advanced materials; for their production, widely used sintering method is one of the main manufacturing processes to obtain composite products applied for high strength, lightweight materials and mainly as high temperature and wear resistance in aerospace and automotive industry.

Recently, the demands for lightweight materials having a high strength and a high toughness have attracted a lot of attention to the development of composite sponge structures and/or composite reinforced with light materials as nonconventional organic materials such as sugar and/or porous ceramic oxides [1–4, 7] one of our papers on cinasite or vemiculite.

The powder metallurgy (PM) route is known as most commonly used method for the preparation of discontinuous reinforced MMCs. This method is generally used as low—medium cost to produce small objects (especially round), tough, the high strength and resistant materials. Since no melting is involved, there is no reaction zone developed, showing high strength properties. For this reason, in the present work, a simple idea was developed on the production of sponge composites by using a low cost method (mixture of aluminum matrix with organic sugar admixing small size glass bubbles and cold pressing + sintering). In reality, Al-alloy based composites were thought during last 20 years in process when the possibilities of improvement in Al alloys by the then conventional methods of heat treatment and microstructural modification had touched its limit. Consequently, new and attractive processes of composites have replaced a prime as compared to the other processes when the cost and simplicity of manufacturing were compared [1–6]. At the first step of this research, a typical porous structure has been created by using organic sugar particulates and an open spaces created by the volatilization of the sugar particulates constitute a net of interrelate porosity in the final product, called a low cost metallic sponge [5–7].

The scope of this work is to identify and investigate the procedures required for a low cost processing route of MMCs containing glass bubbles reinforcements, for engineering applications. The current research uses a simple sintering

F. Gatamorta • M.H. Robert (✉)
Mechanical Engineering Faculty, University of Campinas, Campinas, SP, Brazil
e-mail: fabiog@fem.unicamp.br; helena@fem.unicamp.br

E. Bayraktar (✉)
Mechanical and Manufacturing Engineering School, SUPMECA—Paris, Paris, France
e-mail: emin.bayraktar@supmeca.fr

G. Tandon (ed.), *Composite, Hybrid, and Multifunctional Materials, Volume 4: Proceedings of the 2014 Annual Conference on Experimental and Applied Mechanics*, Conference Proceedings of the Society for Experimental Mechanics Series,
DOI 10.1007/978-3-319-06992-0_2,

technique under inert environment (mainly Argon gas), which has the certain advantages over liquid state methods. Lower processing temperatures decreases the probability of the matrix reacting unfavorably with the reinforcement, improves glass bubbles and organic sugar particle distribution, presents potentially lower energy consumption, simplified operation methods with a low time scale, etc. The work carried out during this present research project has the following overall aims: to develop the understanding of powder metallurgy techniques in producing sponge aluminum metal matrix composites; to make the persistence of the lowering of costs in the processing of these composites.

2.2 Experimental Conditions

2.2.1 Materials and Green Compact

Four different compositions were prepared for the present work: pure aluminum (99.5 %) matrix was mixed with 30 wt% of white sugar granulates (WS) or 30 wt% of Brown Sugar (BS) granulates as two basic compositions; two other compositions were prepared by addition of 10 wt% Glass Bubbles (GB-hollow glass microspheres produced by the company-3M with a density of 0.227 g/cm^3, specified as S38HSS & K1) on the former two compositions. Finally, for sake of simplicity, these four compositions were classified under the name of the following codes:

1. Al + 30 % BS
2. Al + 30 % BS + 10 % GB
3. Al + 30 % WS
4. Al + 30 % WS + 10 % GB

All of the powders used in this work, Al for the matrix and additional elements, were analyzed in a differential thermal analyzer to determine the critical temperature-transformation points (solid–liquid zone) and mass loss *versus* temperature; they had also their size and geometry analyzed by SEM. All compositions were mixed during 4 h in a stainless steel mixer with addition of 2 % Zinc Stearate to facilitate the lubrication. The role of the sugar granulates used in the matrix is to create nearly homogeneous distribution of empty spaces in the matrix during the sintering process. To prepare green compaction of the powder mixtures, a double action-hydraulic press with a capacity of 100 tons was used. For compaction of the mixture, a stainless steel mold with a diameter of 20 mm was used, resulting in green compacts of same size (diameter: 20 mm and height: 30 mm).

2.2.1.1 Sintering

Samples of green compacts were sintered under inert atmosphere with argon gas. The treatment for solid state sintering was carried out in two steps: firstly, the volatilization of the sugar was made at a temperature of 200 °C for a fixed time of 60 min; at the second step the consolidation of sintering was completed at the temperature of 620 °C for a total period of 180 min. Heating rate was 10 °C/min for both steps. During the first step, removing of the sugar must be complete by allowing the gas created by the melting and volatilization of the sugar granulates to scape, resulting in a porous structure with nearly homogeneous porous distribution. This structure is consolidated by the second step sintering.

2.2.1.2 Measurements of the Density and Porosity of the Compacted Specimens Before and After Sintering

All of the measurements of the density and porosity of the specimens were carried out by pycnometry (digital density meters, Webb and Orr, 1997 work with helium gas) before and after sintering and the results were then compared.

2.2.1.3 Mechanical Tests and Microstructural Analyzes

Sintered products were submitted to compression tests, carried out in a servo-hydraulic INSTRON Universal test device (model Instron 5500R, equipped with a load cell of 25,000 kgf) with a quasi-static low speed (initial rate: 10 mm/min and second rate: 5 mm/min rate). Maximum load endpoint was 4,500 N. All testing parameters are given in Table 2.1.

Table 2.1 General conditions for compression tests of produced composites

Initial speed (mm/min)	10	10	10	10
Load endpoint (N)	4,448	4,448	4,448	4,448
Outer loop rate (Hz)	100	100	100	100
Secondary speed (mm/min)	5.08	5.08	5.08	5.08
Strain endpoint (%)	80	80	80	80

Furthermore, dynamic drop tests were carried out on an universal drop weight test device (Dynatup Model 8200 machine) with a total weight of 10.5 kg, punch height of 600 mm and with an impact velocity of 3 m/s.

Microstructure of produced foams was observed by using Scanning Electron Microscopy (JOEL-SEM).

2.3 Results and Discussion

Results of differential thermal analysis of the Aluminum, Glass Bubbles (GB), White Sugar (WS) and Brown Sugar (BS) powders are shown in Fig. 2.1. In the same figure are also presented images of the powders obtained by SEM.

It can be observed in the DTA curves, the critical temperature-transformation points of the different raw materials: a high energy transformation is observed for Al powders around 650 °C (647.5 °C), without mass loss, related to the melting point of the aluminum. For White and Brown Sugar powders, it is observed in DTA curves a significant transformation starting around 180 °C, followed by a heavy mass loss starting round 220 °C; these points can be assumed as melting and volatilization temperatures, respectively. Both sugar powders present the same behavior.

Related to the Glass Bubbles, Fig. 2.2b shows some reaction when heating from room temperature to 140 °C, with around 5 % of mass addition. This can be related to some chemical reaction in the glass material and must be further investigated.

SEM images show aluminum powders with irregular, elongated shape, with average dimensions ranging from 16 to 300 μm. Hollow glass spheres are perfectly rounded, presenting diameters from 3 to 100 μm; White Sugar and Brown Sugar granulates present polygonal morphology and sizes of 200–300 mm and 400–900 mm, respectively.

Table 2.2 summarizes results of measurements of the density and the porosity of the specimens before (green compact) and after sintering (composite). Results show that the density of all the green compact specimens for the four compositions investigated varies between 2.31 and 2.41 g/cm^3. After sintering these values decrease around 50 %, to the levels of 1.61–1.79 g/cm^3. The effect of the presence of the hollow Glass Bubbles and the type of the sugar granulate used, on the product density is not so remarkable and remains inconclusive. While foams produced from Brown Sugar present lower density when Glass Bubbles are added, foams produced from White Sugar present slightly higher density when this additive is incorporated to the structure. Expected result would be decrease in density with GB addition to the material.

Percentages of free space and massive regions were measured in the green compact specimens as 5–7 % and 92–94 % respectively. After sintering free spaces/massive regions ratio increases as the sugar granulates suffer volatilization, at the same levels for all of four compositions. Sintering treatments is found correct for these compositions.

Microstructural analysis of the obtained products was carried out by using Scanning Electron Microscope (SEM). Figure 2.2 shows pictures taken from surface and transversal sections of the specimens WS30GB10 and BS30GB10.

It can be observed the presence of Glass Bubbles distributed in the structure, as well as the free spaces left by the volatilization of the sugar granulates. Thinner cell walls are present when using coarser sugar particles (BS), compared to those obtained for finer sugar particles (WS). Considering the same weight content of sugar, higher amount of total particles is present for the coarser one.

Results of dynamic compression tests (drop test) of the produced foams, are presented in Fig. 2.3, where the behavior of the materials during impact can be compared among the four compositions investigated. Each curve represents the average of results obtained for four tested samples. Compositions WS30 and BS30 without Glass Bubbles present the higher maximum load capacity (26–27 kN) compared to the values obtained (20 kN) for compositions with Glass Bubbles, i.e. BS30GB10 and WS30GB10. However, both compositions with Glass Bubbles show higher plastic deformation and less brittleness regarding to the compositions without Glass Bubbles. It means that the values of the deflection at maximum load for the specimens containing Glass Bubbles are higher compared to those of the specimens without Glass Bubbles. The behavior of each type of foam can be also related to its density: apart of the high density value for the WS30GB10 condition, it seems that maximum load capacity are obtained for products with higher density, as expected for conventional cellular materials. Higher plastic deformation would also be expected, in general, for lower density foams.

Impact energy, total energy and other information obtained from these tests are indicated in Table 2.3. It can be observed significant energy absorption during impact, in all cases. The values obtained are similar for all products tested.

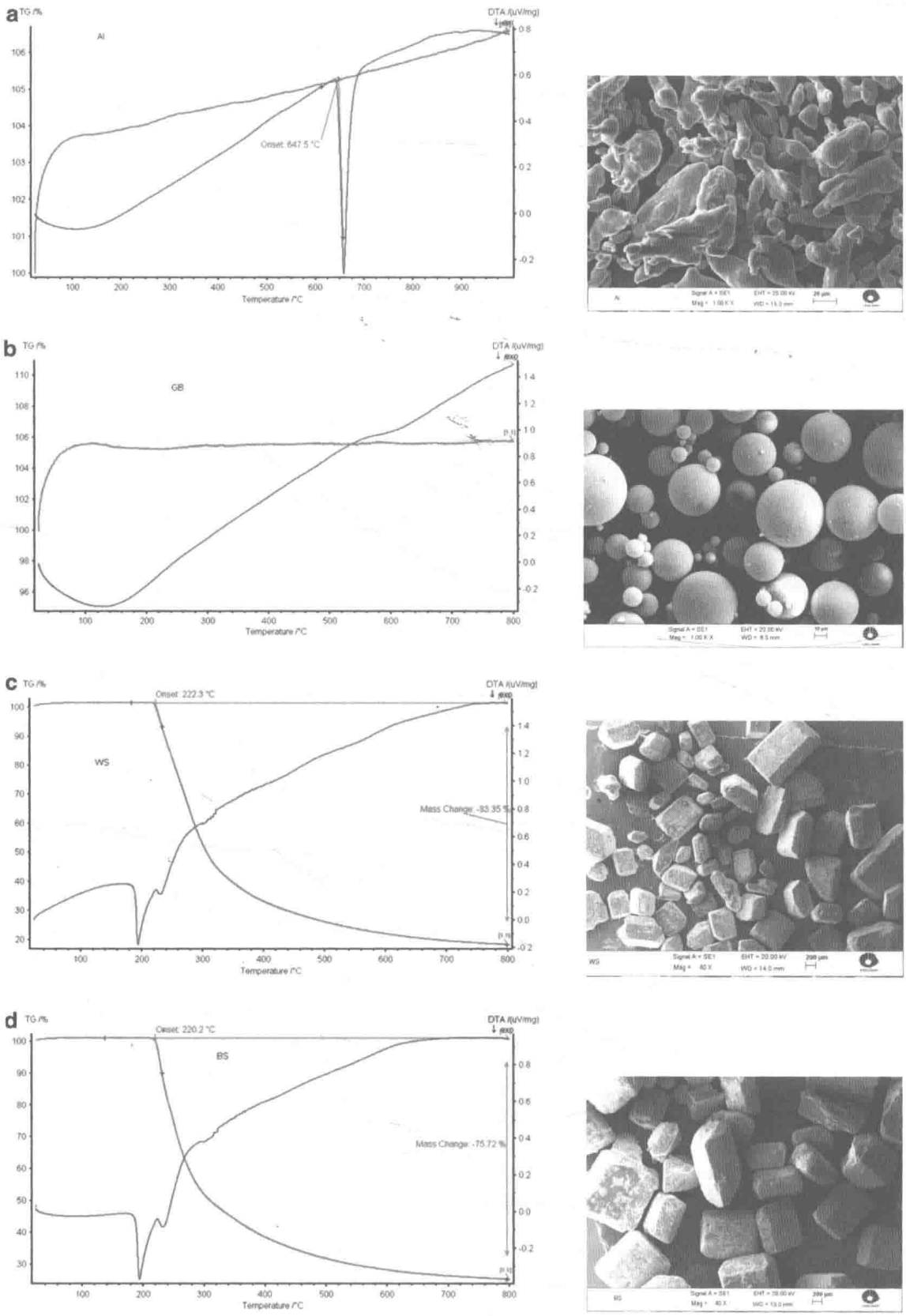

Fig. 2.1 Results of differential thermal analysis (DTA) and thermogravimetry (TG) of the different powders used to produce foams; images by SEM of the corresponding material. (**a**) Aluminum (as matrix), (**b**) glass bubbles (additional element), (**c**) white sugar (space holder) and (**d**) Brown Sugar (space holder)

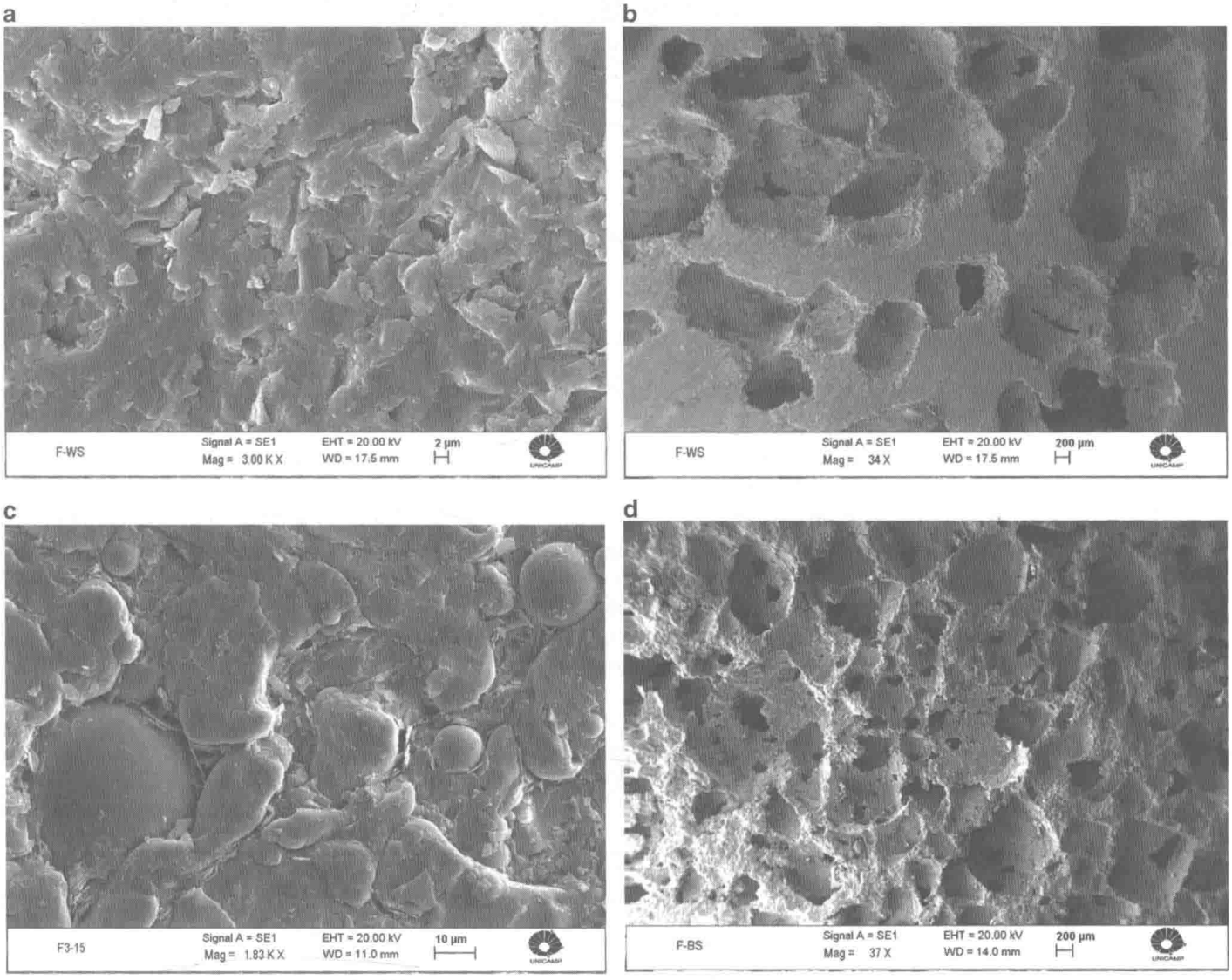

Fig. 2.2 SEM pictures taken from surface and transversal sections of the foams WS30GB10 and BS30GB10. (**a**) WS30GB10; SEM microstructure (surface section), (**b**) WS30GB10; SEM microstructure (transversal section), (**c**) BS30GB10; SEM microstructure (surface section) and (**d**) BS30GB10; SEM microstructure (transversal section)

Table 2.2 Measurements of the density and porosity by He gas pcynometer (digital density meters)

	Condition of specimen	ρ (g/cm^3)	% of empty space	% of massive regions
BS30	Green compact	2.409 ± 0.011	5.42	94.58
	After sintering	1.794 ± 0.025	39.90	60.10
BS3010GB	Green compact	2.358 ± 0.022	5.79	94.21
	After sintering	1.615 ± 0.034	46.39	53.61
WS30	Green compact	2.345 ± 0.010	8.13	92.55
	After sintering	1.713 ± 0.020	42.34	57.66
WS3010GB	Green compact	2.314 ± 0.009	7.93	92.08
	After sintering	1.740 ± 0.022	41.68	58.32

Figure 2.4 shows results of semi-static compression tests for all of the four compositions investigated. Evolution of the stress values depending on the deformation (strain levels as %) were compared with different parameters, for example, peak values (stress as MPa) are found similar levels (45 MPa) for three compositions but only the specimens called BS30 have given much more higher values, around 97 MPa (quasi double). Other test results were summarized in Table 2.4.

From both sorts of compression tests, it seems that the role of Glass Bubbles is relevant on the plasticity of the composites and they give better ductility if they are added in the matrix up to 10–15 %. Some of the test results not given